Article

Protein Sci
DOI10.1002/pro.3905

(*S*)-4-Amino-5-phenoxypentanoate Designed as a Potential Selective Agonist of the Bacterial Transcription Factor GabR

Running Title: Design a Potential Selective Agonist of GabR

Daniel S. Catlin[1§], Cory T. Reidl[1§], Thomas R. Trzupek[2], Richard B. Silverman[2,3], Brian Cannon[4], Daniel P. Becker[1*], and Dali Liu[1*]

[1]Department of Chemistry and Biochemistry, Loyola University Chicago, 1032 West Sheridan Road, Chicago IL 60660, USA; [2]Department of Chemistry, Chemistry of Life Processes Institute, Center for Molecular Innovation and Drug Discovery, [3]Department of Molecular Biosciences, Northwestern University, 2145 Sheridan Road, Evanston, IL 60208-3113, USA; [4]Department of Physics, Loyola University Chicago, 1032 West Sheridan Road, Chicago IL 60660, USA.

[§]These authors contributed equally.

*To whom correspondence should be addressed: Dali Liu, Department of Chemistry and Biochemistry, Loyola University Chicago, IL 60660, dliu@luc.edu, 773.508.3093

or Daniel P. Becker: Loyola University Chicago, Department of Chemistry and Biochemistry, dbecke3@luc.edu, 773.508.3089

Manuscript Pages: 35
Supplemental Pages: 7
Tables: 1
Figures: 5
Schemes: 2
Supplemental Material: contains material and methods for organic synthesis of a series of analogs of (*S*)-4-amino-5-phenoxypentanoate (4-phenoxymethyl-GABA), which is detailed in main body, as well as figures to complement the discussion in the main text.

Received: May 07, 2020;Revised: Jun 12, 2020;Accepted: Jun 16, 2020

Abstract

Addressing molecular recognition in the context of evolution requires pursuing new molecular targets to enable the development of agonists or antagonists with new mechanisms of action. Disruption of transcriptional regulation through targeting transcription factors that regulate the expression of key enzymes in bacterial metabolism may provide a promising method for controlling the bacterial metabolic pathways. To this end, we have selectively targeted a bacterial transcription regulator through the design and synthesis of a series of γ-aminobutyric acid (GABA) derivatives, including (*S*)-4-amino-5-phenoxypentanoate (4-phenoxymethyl-GABA), which are based on docking insights gained from a previously-solved crystal structure of GabR from *Bacillus subtilis*. This target was selected because GabR strictly controls GABA metabolism by regulating the transcription of the gabT/D operon. These GabR transcription modulators are selective for the bacterial transcription factor GabR and are unable to bind to structural homologs of GabR due to distinct steric constraints. We have obtained a crystal structure of 4-phenoxymethyl-GABA bound as an external aldimine with PLP in the effector binding site of GabR, which suggests that this compound is capable of binding and reacting in the same manner as the native effector ligand. Inhibition assays demonstrate high selectivity of 4-phenoxymethyl-GABA for bacterial GabR versus several selected eukaryotic enzymes. Single-molecule fluorescence resonance energy transfer (smFRET) experiments reveal a ligand-induced DNA distortion that is very similar to that of the native effector GABA, suggesting that the compound functions as a potential selective agonist of GabR.

Keywords: Bacterial transcriptional regulation, MocR, GabR, PLP, structure-based ligand design, DNA distortion, X-ray crystallography, single-molecule FRET, organic synthesis.

This research demonstrates the design and synthesis of a tight-binding and potential selective agonist of the transcriptional regulator GabR in non-pathogenic *Bacillus subtilis*, and thus opens the door to the possibility of specifically targeting the modulation of bacterial transcription. Analysis of the effects of a new and selective ligand is explored through the use of biochemical techniques, including X-ray crystallography and enzymatic assays, in conjunction with the biophysical technique single-molecule FRET. The manuscript proves the concept in designing and synthesizing modulators of the transcriptional regulator GabR in key bacterial metabolism pathways.

Abbreviations:

GABA: γ-aminobutyric acid

GABA-AT: GABA-aminotransferase

SSDH: succinate semialdehyde aminotransferase

wHTH: winged helix-turn-helix

eb/o: effector binding/oligomerization

Asp-AT: aspartate aminotransferase

PLP: pyridoxal-5'-phosphate

GAD: glutamate decarboxylase

OAT: ornithine aminotransferase

Ala-AT: alanine aminotransferase

smFRET: single-molecule Förster resonance energy transfer

FRET: Förster resonance energy transfer

INTRODUCTION

In *B. subtilis*, the gabT/D operon [Fig. 1(a)] encodes the genes responsible for γ-aminobutyric acid (GABA) catabolism including GABA aminotransferase (GABA-AT), which is the product of the gabT gene, and succinate semialdehyde dehydrogenase (SSDH), which is the product of the gabD gene. Transcription of enzymes in this metabolic pathway is strictly regulated by the transcription regulator GabR (UNIPROT: P94426), a member of the MocR/GabR subfamily of the GntR family of transcription factors.[1-3] GabR forms a head-to-tail homodimer in solution and has high sequence homology to type-I aminotransferases. Each subunit of GabR consists of an *N*-terminal winged helix-turn-helix (wHTH) DNA-binding domain and a *C*-terminal effector-binding/oligomerization (eb/o) domain [Fig. 1(b)] homologous to highly conserved Type-I aminotransferases, such as GABA-AT and aspartate aminotransferase (Asp-AT).[2-4]

In 2015, *Wu et al*. reported that GabR facilitates a "partial" aminotransferase-like reaction involving GABA and the cofactor pyridoxal-5'-phosphate (PLP), forming an external aldimine. However, GabR is incapable of completing the "Ping-Pong" transamination reaction due to

conformational restraints imposed by Tyr 281.[4] As a result, GabR functions solely as a PLP-dependent transcriptional regulator, responding to the concentration of GABA but without catalytic capacity.[4] The current GabR-DNA binding model suggests that GabR binds as a homodimer to regulate transcription. GabR specifically recognizes GABA, which induces protein conformational changes upon binding.[5-7] The changes in protein conformation are believed to result in DNA distortion, thereby activating transcription of the gabT/D operon.[4–7] The specific recognition of GABA by GabR as opposed to α-amino acids is critical to ensure activation of the gabT/D operon only when needed, and is particularly important in the bacterial stress response and survival. The importance of selectivity for GABA was revealed by gabR, gabT, and gabD gene knockout studies in *B. subtilis*, which resulted in mutated organisms that were incapable of utilizing GABA as their sole carbon/nitrogen source. Moreover, GabR has been shown to be sensitive to increased intracellular GABA concentrations.[1,2]

To regulate gene expression, an organism may exercise control directly at the site of transcription.[8,9] Through transcription regulation, both *E. coli* and *B. subtilis* control metabolic pathways responsible for acid elimination in response to low pH environments, albeit via different mechanisms.[10-12] Under acidic stress conditions, some bacteria, including *E. coli*, can maintain pH homeostasis by consuming intracellular glutamate via the glutamate decarboxylase (GAD) reaction. The GAD reaction eliminates one intracellular proton and in conjunction produces one GABA molecule that is exported from the intracellular space via the antiporter GadT2. However,

this pathway requires the GABA shunt pathway to relinquish the key nitrogen source glutamate, and glutamate depletion is detrimental to bacteria.

The role of the gabT/D operon in *B. subtilis* appears to function similarly to the GABA shunt pathway in *E. coli* under acidic stress. This would place GabR in a key role affecting the ability of *B. subtilis* to survive in acidic environments, thus making this protein a viable target to manipulate the pH homeostasis stress response in bacteria. With the ultimate goal of developing a new class of bacterial gabT/D transcription modulators, we have synthesized a series of aryl-functionalized GABA derivatives, including (*S*)-4-amino-5-phenoxypentanoate (referred to hereafter as 4-phenoxymethyl-GABA), that were designed to specifically target the binding site of GabR based on a known crystal structure of GABA (PDB: 5T4J). We have obtained a 2.75 Å resolution protein-ligand complex structure of 4-phenoxymethyl-GABA bound as an external aldimine (4-Phenoxymethyl-GABA-PLP, hereafter referred to as PGP) in the eb/o domain of GabR. Selectivity of this compounded was probed against other PLP-dependent enzymes including GABA-AT, ornithine aminotransferase (OAT), alanine aminotransferase (Ala-AT), and Asp-AT, finding little-to-no inhibition. To probe possible effects of 4-phenoxymethyl-GABA on GabR-mediated transcription in bacteria, we conducted single-molecule Förster resonance energy transfer (smFRET) experiments to examine DNA distortion induced by the binding of 4-phenoxymethyl-GABA.

RESULTS

Chemistry. Tosylate **2** was prepared as outlined in Scheme 1 from commercially available lactam **1** by reaction with p-toluenesulfonyl chloride in the presence of triethylamine and a catalytic amount of *N*,*N*-dimethylaminopyridine (DMAP). Aryloxy- and arylthiolactams **8**-**12** were prepared through nucleophilic substitution by nucleophiles **3**-**7** with potassium carbonate in refluxing acetonitrile over a 20-hour reaction period. Lactam intermediates **8**-**12** were then each individually treated with 6 M HCl under reflux to produce the final aryloxy-GABA derivatives (**13**-**17**) in quantitative or nearly quantitative yields. In most cases, final compounds were obtained directly from the hydrolysis in purities greater than 95%. Further purification was achieved via reverse phase flash chromatography where specified.

Crystallography. A crystal of truncated (positions 107-471) holo GabR was soaked overnight with 4-phenoxymethyl-GABA **13**. An X-ray crystal complex structure of **13** and PLP as an external aldimine bound to the eb/o domain of GabR was solved by molecular replacement using a dimer from a previously reported truncated structure of GabR (PDB code: 5T4J) after deletion of all water molecules and ligand atoms. In space group $P4_12_12$, one asymmetric unit contained 4 monomers. Two monomers form one homodimer as a truncated biological assembly (with the wHTH domain deleted), and there are two truncated biological assemblies in one asymmetric unit. The final model was refined to a resolution of 2.75 Å with a R_{free}/R_{work} values of 20.18%/17.31%, respectively. Final refinement statistics are reported in Table 1. The solved structure of GabR-PGP has been deposited in the PDB as (PDB code: 6UXZ).

After molecular replacement, the experimental map (F_o-F_c) showed electron density in the binding site that could not be attributed to PLP alone, demonstrating the presence of the ligand 4-phenoxymethyl-GABA, bound as an external aldimine formed between PLP and **13**, and termed PGP. In the refined model [Fig. 2(a)], hydrogen bonds were observed between Arg 207 (3.4 Å), His 114 (2.7 Å), Arg 430 (2.5 Å), and the carboxylate of PGP [Fig. 2(a)]. A superimposition of external aldimine PLP-GABA and external aldimine PGP highlights the unique space occupied by the phenoxyl substituent [Fig. 2(b)]. A polder map (F_o-F_c) of the external aldimine was generated by removing PGP, as shown in Figure 3.

Off-Target Screening. The eb/o domain of GabR type bacterial transcription regulator are homologous and structurally similar to PLP-dependent aminotransferases including those in eukaryotes. To screen for potential off-target activity and to ascertain the potential of our 4-phenoxymethyl-GABA as a selective GabR agonist in bacteria without interaction with mammalian enzymes, four important PLP-dependent human aminotransferase enzymes, known to have off-target inhibition potential when targeting a PLP-dependent protein, were selected, including GABA-AT, Asp-AT, Ala-AT and OAT. These enzymes were selected because all four utilize the same co-factor (PLP), follow similar enzymatic reaction mechanisms, and represent the general molecular recognition employed by PLP-dependent aminotransferases. They are commonly used to test the selectivity of synthesized covalent inactivators against PLP-dependent aminotransfeases.[13-15] At the three concentrations tested, modest inhibition was only observed at the highest concentration of 5.0 mM (Fig. 4). The conducted off-target screen also proves a

concept that designed ligand displays potential to treat bacterial pathogens that rely on GabR-mediated transcription regulation for virulence or survival in the future.

*Effects of **13** on oligomerization and DNA distortion*. To test the effect of 4-phenoxymethyl-GABA (**13)** as a potential agonist of GabR that may promote transcription, the transcription activation signal in the DNA caused by GABA needed first to be elucidated. To this end, smFRET experiments were performed using a 53 base-pair (bp) fragment of the GabR-DNA binding region. A GabR-DNA binding model was generated based on SAXS data in an early publication and was generously provided by Dr. Till Boecking at New South Wales University, Australia via personal communication.[5] Using this GabR-DNA complex model as a guide (Fig. S2), fluorescent dyes (Cy3-donor and Cy5-acceptor) were positioned 19 bp apart (Fig. S2), so that changes in the DNA structure could be detected via FRET signals correlating to the distance between the two fluorophores.

For immobilized DNA constructs in the absence of GabR, smFRET time traces for individual molecules exhibited an exclusively low FRET signal (Fig. S3). Histograms generated from the accumulated behavior of the observed molecules were well fit by a single-peak, having a Gaussian distribution with an average FRET (<FRET>) value of 0.23 [Fig. 5(a)]. This FRET value is consistent with the expected distance between Cy3 and Cy5 fluorophores positioned 19 bp apart on opposing strands (Table S2). For DNA preincubated with GabR prior to immobilization, the time traces displayed two distinct FRET states: a low FRET state consistent with free DNA, and a

distinctly higher FRET state. The smFRET histogram for the GabR-DNA complexes have a bimodal distribution [Fig. 5(b)]. Analysis by Gaussian fitting yielded two peaks with <FRET> values of 0.26 and 0.48 (Table S1). Extended observation did not detect any conversion between the two FRET distributions, indicating that these FRET values represent two distinct populations. The low FRET population was thus assigned to free DNA, and the high FRET population represents the GabR-DNA complex. The increased FRET level for the GabR-DNA complex suggests that GabR binding to DNA induces a bent conformation, perhaps through local melting within the linker region. This observation provides direct evidence of GabR modulating DNA conformation and supports structural studies that modeled a bent DNA conformation for the GabR-bound state. The time traces for the GabR-DNA complexes did not exhibit any detectable transitions, indicating that the complex is stably formed with the DNA held in a static, nonlinear orientation with no switching between conformations.

The high FRET state associated with the GabR-DNA complex provides a signal for the inactivated complex and serves as a reference for testing whether addition of activating ligands, such as GABA, will induce further conformational change in the GabR-DNA complex for the activation state. Indeed, addition of GABA to GabR-DNA shifted the FRET distribution to a lower value, <FRET> = 0.32 as shown in the smFRET histograms (Figure 5c) and the time traces (Figure S3). The lower FRET state suggests that GABA binding relaxes the bent conformation or induces an out-of-plane distortion. Similarly, addition of **13** to GabR-DNA lowered the <FRET> value to

0.41 [Fig. 5(d)], consistent with the model that **13** acts as an agonist by occupying the GABA-binding pocket and inducing some local distortion in GabR-bound DNA.

Although distance is only one of many factors that can cause changes in FRET, interdye distances calculated from average FRET values can provide useful insight into how GabR and its effectors alter the conformation of the bound DNA. Based on prior SAXS results indicating that bound DNA wraps around GabR, the interdye distances were interpreted via a multi-segmented geometric model for the DNA conformation (Fig. S4). From this model, estimates of the bend angles induced by GabR binding were calculated (Table S2). The unbound DNA had an interdye distance of 6.6 nm, which yields a bend angle of 0° and is consistent with a 19-bp dye separation. GabR binding to DNA reduced the interdye distance to 5.5 nm, which corresponds to a DNA bend angle of 47°. The structural information for the bound DNA gleaned from the smFRET experiments complements the SAXS-derived, global structure of GabR to provide a more complete picture of the GabR-DNA complex.[5] In the presence of GABA, the interdye distance increased to 6.1 nm, suggesting either relaxation of the DNA bending or out-of-plane twisting to further separate the dyes.

DISCUSSION

In their findings, *Wu et al.* concluded that GabR is incapable of catalyzing a transamination reaction and that GabR is only able to facilitate the formation of the external aldimine.[4] In addition, a synthesized GABA derivative (*S*)-4-amino-5-fluoropentanoic acid (AFPA) was proven to be an

agonist of GabR, activating transcription of the gabT/D operon. Compared to GABA, AFPA resulted in greater activation *in vitro*, although AFPA yielded lower activation *in vivo*.[4] GABA permease (GabP), a transmembrane protein responsible for the translocation of external GABA to within the cell, may have low affinity for AFPA and be the cause of the discrepancy. Given that AFPA was able to react similarly to GABA and activate transcription, this molecule was chosen as the lead compound in this research to be further optimized. Improving selectivity toward GabR was an important first step in the molecular probe design process. To validate and further improve ligand design, the GabR-PLP-GABA co-crystal structure was explored to identify structural characteristics unique to the GabR binding site. It was observed that GabR possesses a hydrophobic pocket that is not found in the active sites of other PLP-dependent enzymes, including GABA-AT, Asp-AT, and OAT. On this basis, we used a known GabR agonist AFPA as a molecular probe for GabR to examine the transcription factors binding site reactivity.[4] It was hypothesized that aryloxyl- and arylthio moieties could replace the fluorine of AFPA and result in increased binding affinity to GabR by forming additional stabilizing contacts in this hydrophobic pocket in the GABA binding site while sterically excluding off-targets. To this end, we have synthesized several aryloxyl- and arylthio derivatives, as summarized in Scheme 1.

The distances in the GabR-PGP structure deviate only slightly from the GabR-PLP-GABA co-crystal structure [Fig. 2(b)]. These residues facilitate recognition of monocarboxylate ligands, such as the native effector GABA, as well as synthetic GABA derivatives, such as AFPA, and facilitate Schiff base formation with PLP. Formation of the Schiff base has been reported as the

chemical reaction responsible for the GabR mediated transcription activation of the gabT/D operon.[4] In addition, the conserved interactions between the phosphate group of PLP and Tyr 181, Thr 309, Ser 311, Arg 319, and Ser 321, more commonly referred to as the "phosphate-binding cup" for PLP dependent enzymes, were also observed in the GabR-PGP crystal structure, and these interactions prevent co-factor displacement.[4]

As seen in Figure 2(a) the O3 atom of PGP and the acidic proton of Tyr 281 are within hydrogen bonding distance (3.1 Å). This interaction is absent in the GabR-PLP-GABA co-crystal structure (PDB code: 5T4J) because a hydrogen bonding acceptor does not exist in the PLP-GABA external aldimine at the same position. The additional hydrogen bond likely further increases selectivity and affinity of PGP compared to GABA alone in formation of the external aldimine of PLP-GABA. It will be of interest to investigate any difference in binding or affinity with the replacement O3 in **13** to an atom incapable of hydrogen bonding, such as in the arylthio analogue **17**. A polder (omit) map[16] shown in Figure 3 (F_o-F_c at 3.0σ) superimposed with PGP from the GabR binding site further supported the formation and position of the external aldimine between PLP and **13** [Fig. 2(a)].

To elucidate why the 4-phenoxymethyl-GABA derivative **13** is selective against the off-target enzymes, the active sites from the inhibited structures of these off-targets were used to visualize how PLP-**13** (PGP) compared to the positions of the inhibitor complex in the enzyme's active sites. The PLP moieties were manually structurally aligned in Chimera and the van der Waals radii of PGP were represented as a surface feature (Fig. S1). It was observed that PGP would

encounter unfavorable interactions within the active sites of these off-target enzymes. Either the side chain residues or the backbone of the active sites clashed with the surface feature of PGP. These unfavorable interactions should preclude **13** from binding to these off-target enzymes and is the reasoning for the observed limited inhibition. As proposed, the phenoxyl moiety of **13** includes additional steric bulk that limits off-target inhibition.

Proposed mechanisms for transcription regulation include direct interactions between activators and RNA polymerase, or as is suspected for GabR, activators may induce DNA distortion that reposition promoters in more favorable orientations to interact with RNA polymerase.[17-20] We hypothesize a mechanism for GabR wherein GabR limits the promoter-RNA polymerase interactions necessary for transcription during DNA oligomerization. Next, binding of GABA within the eb/o domain induces protein conformational changes resulting in DNA distortion resulting in the necessary promoter-RNA polymerase interactions being restored, and transcription of the gabT/D operon is activated.

Given that transcription is only activated in the presence of an effector ligand such as GABA, the FRET distribution in the presence of a ligand was expected to be distinguishable from both free DNA and GabR-DNA complex. Indeed, the FRET distribution in the presence of GABA was unique and intermediate to the values of free and GabR-DNA complex. This observation suggests that 1) DNA is initially distorted during oligomerization with GabR and that 2) DNA undergoes further distortion during the protein conformational changes induced by GABA. A lower <FRET> value suggests that DNA distortion caused by GABA is a relaxation in the

curvature of the DNA; however, twisting in the DNA strand could also promote activation. This twisting-based activation could originate from the manner in which DNA wraps around GabR, with positive charges following an "S" type of shape along the surface of GabR. Various groups have reported similar findings regarding the GabR-DNA complex in the presence of GABA.[5-7,21] The results in this report are consistent with the findings of Al-Zyoud, whose group was the first to suggest that the DNA wraps around GabR during oligomerization and that the addition of GABA results in a larger overall complex structure of GabR.[5] It was proposed that the larger complex structure would cause the bending in the natural curvature of the DNA to decrease, thus activating transcription.[5] Similar DNA distortion mechanisms had been previously observed in the well-studied MerR family of transcription factors. These proteins bind between the -35 and -10 elements, activating suboptimal promoters by contracting DNA in response to external stimuli.[22-25] Even though the -35 element of the gabT promoter is positioned within the GabR binding site, it does not play a role during oligomerization and is free to interact with RNA polymerase. A similar effect on DNA distortion and <FRET> values would be expected if 4-phenoxymethyl-GABA **13** functions as an agonist of GabR. Similar to GABA, **13** caused the <FRET> distribution to decrease in between the values of free and oligomeric DNA, indicating that **13** elicits a comparable effect on DNA distortion.

Conclusion

The novel synthetic GABA derivative, (*S*)-4-amino-5-phenoxypentanoate (**13**) and related analogs were designed to selectively bind to GabR and thereby to potentially modulate transcription induced by GabR, and these studies demonstrate that **13** can potentially functions as a GabR agonist. A crystal structure of truncated GabR with **13** revealed the formation of an external aldimine between **13** and the cofactor (PLP) in the binding site. smFRET studies support an agonistic response elicited by **13** that is similar to the native effector ligand, GABA, via DNA distortion. The distortion of DNA is necessary to activate transcription of the gabT/D operon. Furthermore, *in vitro* studies indicate that **13** is selective toward GabR with very limited inhibition of off-target human aminotransferases.

MATERIALS AND METHODS

Anhydrous solvents (THF, CH_2Cl_2, MeOH, Et_3N, and DMF) were distilled prior to use. All other solvents, reactants, and reagents were purchased from commercial vendors and were used without further purification. Melting points were determined in capillary tubes using a Büchi melting point B-540 apparatus and are uncorrected. ^{1}H-NMR spectra were recorded at 500 MHz, using a Bruker Avance III 500 (direct cryoprobe), and ^{13}C-NMR spectra were obtained at 126 MHz using the same instrument. High-resolution mass spectral data were obtained at the Integrated Molecular Structure Education and Research Center (IMSERC, Northwestern University) on an Agilent 6210A TOF mass spectrometer in positive ion mode coupled to an Agilent 1200 series

HPLC system. Data were processed using MassHunter software version B.04.00. Flash column chromatography was performed using an Agilent 971-FP automated flash purification system with a Varian column station and SiliCycle cartridges (12-80 g, both normal and High Performance). Analytical HPLC was performed using an Agilent Infinity 1260 HPLC system and injection volumes of 5-10 μL. A Phenomenex Luna 5 μm C-8(2) 100 Å column, 50 x 4.60 mm, was used for all HPLC experiments, using a 10-minute gradient of 95% H_2O/5% acetonitrile + 0.05% TFA to 95% acetonitrile/5% H_2O + 0.05% TFA, at 1.5 mL/min. The purity of all final target compounds was found to be ≥95% by HPLC. Analytical thin-layer chromatography was performed on Silicycle extra-hard 250 μm TLC plates. Compounds were visualized with short-wavelength UV light, and with ninhydrin or with phosphomolybdic acid, where appropriate.

(S)-(5-Oxopyrrolidin-2-yl)methyl 4-Methylbenzenesulfonate (2) Synthesis: To a stirred solution of (*S*)-5-(hydroxymethyl)-2-pyrrolidinone **7** (1.10 g, 9.56 mmol) and *p*-toluenesulfonyl chloride (1.83 g, 9.59 mmol) in CH_2Cl_2 (22 mL) at 0°C was added DMAP (117 mg, 0.96 mmol) and Et_3N (2.68 mL, 19.2 mmol). The resulting mixture was allowed to warm to 23°C and stirred for 20 h. The reaction was then quenched with water (40 mL), and the aqueous layer was extracted with CH_2Cl_2. The combined organic extracts were washed with 1 M HCl and dried over anhydrous Na_2SO_4. Removal of solvent under reduced pressure followed by dry load flash chromatography purification (1/99 MeOH-EA as the eluent) yielded **1** as a white solid (2.37 g, 92%): mp 128.5-133.5°C, ^{1}H NMR (500 MHz, $CDCl_3$) δ 1.75-1.80 (m, 1H), 2.19-2.35 (m, 3H), 2.44(s, 3H), 3.85-

3.92 (m, 2H), 4.00-4.03 (m, 1H), 6.49 (s, 1H), 7.35 (d, 2H, J = 8.0 Hz), 7.77 (d, 2H, J = 8.1 Hz); ^{13}C NMR (100 MHz, $CDCl_3$) δ 21.6, 22.7, 29.2, 52.5, 71.9, 121.9, 130.0, 132.3, 145.3, 178.2. HRMS (ESI) calculated for $C_{11}H_{15}NO_3$ $[M+H]^+$ 210.1125, found 210.1125. HPLC purity = 99% pure.

General Procedure 1: Nucleophilic displacement of tosylate 2 by phenol and thiophenol derivatives. To a 20 mL dram vial charged with **2** and K_2CO_3 (5.0 eq.) was added dry acetonitrile (0.3M) followed by an excess amount of phenol or thiophenol derivative (3.0 eq.). The reaction vessel was sealed under argon and sonicated for 2 min before stirring at 110°C overnight under an inert atmosphere. HPLC and TLC analysis with PMA staining were used to monitor consumption of starting material. Once the starting material disappeared, the reaction mixture was cooled and partitioned between EtOAc (10 mL) and H_2O (10 mL). The layers were separated, and the aqueous phase was extracted with EtOAc (3 x 5 mL). The organic fractions were combined, dried over anhydrous sodium sulfate, and concentrated. Purification, if necessary, is described below under subheadings for individual compounds.

(S)-5-(Phenoxymethyl)pyrrolidin-2-one (8).

The title compound was obtained according to the general procedure described above starting from tosylate **2** (0.420 g, 1.57 mmol) and phenol (0.249 g, 2.65 mmol). Purification by flash column chromatography (silica gel; gradient from 5% EtOAc/hexane to 100% EtOAc over 10 min, then 100% EtOAc for 10 min) gave lactam **8** (0.227 g, 75% yield) as a white fluffy solid: mp 73-77°C; ^{1}H NMR (500 MHz, chloroform-*d*) δ 7.34 – 7.23 (m, 2H), 6.98 (td, *J* = 7.4, 1.1 Hz, 1H), 6.92 – 6.83 (m, 2H), 6.18 (s, 1H), 4.17 – 4.02 (m, 1H), 3.99 (dd, *J* = 9.2, 3.9 Hz, 1H), 3.82 (dd, *J* = 9.1, 7.8 Hz, 1H), 2.52 – 2.25 (m, 3H), 1.99 – 1.83 (m, 1H); ^{13}C NMR (126 MHz, $CDCl_3$)

δ 177.81, 158.27, 129.59, 121.41, 114.48, 71.28, 53.28, 29.53, 23.15; HRMS (ESI) calcd for $C_{11}H_{14}NO_2$ $[M+H]^+$ 192.1021, found 192.1019; HPLC purity = 98% pure.

General Procedure 2: Hydrolytic Pyrrolidine Ring Opening: A measured amount of the purified pyrrolidine derivative was added to a small dram vial alone with a stir bar. Then a 1-2 mL amount of 6 M $HCl_{(aq.)}$ was added to the reaction vessel followed by degassing and sealing with parafilm. The reaction vial was then heated at 115°C for 2-3 h. The reaction was monitored using TLC and HPLC (method A). Once the starting material was consumed, the reaction vial was heated at 80°C under reduced pressure to remove solvents and crystallize the HCl salt product which was dried overnight in vacuo.

(S)-4-Amino-5-phenoxypentanoic acid hydrochloride (13)

The title compound was obtained according to the general procedure described above starting from lactam **3** (88 mg, 0.458 mmol). Purification by flash chromatography (C18-silica gel; isocratic 100% H_2O elution) gave 4-phenoxymethyl-GABA **13** (49 mg, 43% yield) as a white solid: mp 155.6-160°C; ^{1}H NMR (500 MHz, d_6-DMSO) δ 12.12 (bs, 1H), 8.40 (bs, 3H), 7.32 (t, J=8.7Hz, 2H), 7.00 (d, J=8.4Hz, 3H), 4.15 (dd, J=36.3, 10.2Hz, 1H), 4.12 (dd, J=36.3, 10.2Hz, 1H), 3.52 (m, 1H), 2.47 (m, 1H), 1.94 (m, 2H); ^{13}C NMR (500 MHz, d6-DMSO) δ 173.68, 157.84, 129.51, 121.23, 114.74, 67.01, 49.41, 29.49, 24.70; HRMS (ESI) calcd for $C_{11}H_{15}NO_3$ $[M+H]^+$ 210.1125, found 210.1125; HPLC purity = > 99% pure.

Protein Purification: For protein expression and purification, *E. coli* BL21(DE3) competent cells were transformed with pET24-GabR-eb/o and stored as a glycerol stock. A starter culture in Luria-

Betrani (LB) medium (50 mL) containing kanamycin (50 μg/mL) grown overnight at 37°C and shaken at 250 rpm was used to inoculate a 2 L (50-fold dilution) of LB medium supplemented with kanamycin (50 μg/mL). The expression culture was grown at 37°C, 250 rpm until $OD_{600} \approx 0.6$, then cooled to 4°C for 1 h before induction with isopropyl β-D-1-thiogalactopyranoside (0.5 mM). After the culture was incubated for an additional 16-18 h at 25°C and shaken at 200 rpm, cells were harvested with 3 rounds of centrifugation at 28048 × g for 15 min. The cell pellet was flash frozen in liquid nitrogen for subsequent storage at -80°C.

Cell pellets were resuspended in Buffer A (1X PBS Buffer, 15 mM imidazole, 100 uM PLP, pH 8.5) and lysed by sonication (5 min) alternating 10 s bursts and 20 s rests (Thermo Fisher Sonic Dimembrator 500, 30% amplitude, microtip). Cell debris was removed by centrifugation at 31,000 × *g* for 1 h. The remaining supernatant was subjected to Ni^{2+} affinity chromatography using a HisTrap FF column (GE Healthcare) pre-equilibrated with Buffer A. Protein was eluted using a linear gradient with Buffer B (from 5 mM to 250 mM imidazole, supplemented with 2X PBS Buffer, 100 uM PLP, pH 8.5). Fractions containing protein, identified by observing absorbance at 280 nm, were pooled together and subjected to size exclusion chromatography (HiLoad 16/60 Superdex 200 pg; GE Healthcare) using gel filtration Buffer (Buffer B with 300 mM imidazole). A single eluting peak was observed during this purification step and fractions containing protein were pooled together. Both an aliquot from the Ni^{2+} affinity column eluate and from the final purified truncated GabR protein appeared homogenous when characterized by a Coomassie-stained 12% SDS-PAGE gel. Protein concentrations were measured using the

Bradford assay (BioRad) with bovine serum albumin standards.

Protein Crystallization: For crystallization experiments, protein solution was buffer exchanged with Buffer A. Crystals of truncated GabR were obtained via hanging drop vapor diffusion by mixing 2.5 uL of (10 mg/mL) protein solution with 2.5 uL of well solution (10% PEG 3350, 100 mM imidazole pH 8.0, and 200 mM Li_2SO_4). Crystals were allowed to grow at room temperature and reached optimal size and morphology for data collection after 7-10 days. Truncated GabR (eb/o domain) crystals were then soaked overnight in well solution supplemented with compound **13** (25 mM). Soaked crystals were transferred to the well solution supplemented with 30% PEG400 as cryo protectant and flash frozen in liquid N_2.

Data Collection and Processing: Monochromatic data was collected at Beam Line 19-BM at the Structural Biology Center (SBC), Advanced Photon Source (APS), Argonne National Laboratory (ANL). Diffraction data was collected at a wavelength of 0.98 Å at 100 K using a ADSC 315r Charged Couple Device (CCD) detector. Data sets were indexed and integrated using iMosflm and scaled with SCALA both in the CCP4 software suite.[26] Data statistics are summarized in Data Table 1.

Model Building and Refinement: The GabR-PGP structure was solved by molecular replacement using PHASER in the Phenix software suite.[27] The first search model was based on a previously

published structure of the truncated GabR eb/o domain (PDB Code: 5T4J). The model was rebuilt using COOT,[28] refined using CCP4 and analyzed in COOT and USCF Chimera.[29] All ligands were built and regularized using JLigand in the CCP4 program suite. Final refinement statistics are reported in Table 1. Structural figures were made in USCF Chimera.

Human Aminotransferase Assay Panel: All reagents were purchased from Sigma-Aldrich (St. Louis, MO, USA). Recombinant human pyrroline-5-carboxylate reductase 1 was purchased from Creative Biomart. GABA-AT was isolated and purified from freshly harvested pig brain according to a published procedure.[30] OAT was cloned, expressed, and purified according to a published procedure.[31] Literature procedures were used to determine the inhibition of GABA-AT,[32] human OAT,[33] *L*-aspartate aminotransferase,[34] and *L*-alanine aminotransferase[34] by the GABA analogues. Assays were recorded on a Synergy H1 hybrid multi-mode microplate reader (Biotek, USA), with transparent 96 well plates. All assays were performed in duplicate.

Single-molecule Fluorescence Resonance Energy Transfer (smFRET) Imaging: Single-stranded oligonucleotides (Integrated DNA Technology Inc., Coralville, IA) containing internal Cy3 and Cy5 fluorescence probes inserted as base substitutions were designed based on the GabR binding region.

Forward sequence:
5'-
TCTGATACCATCAAAAAGATTATAATTGGTA/iCy5/CTTTTCATCATACCAAAGATTATAATTT
TCA-3'-Biotin

Reverse sequence:
5'-
TGAAAATTATAATCTTTGGTATGATGAAAAGATACCAATTATAA/iCy3/CTTTTTGATGGTATC
AGA-3'

The 3' of the forward sequence was biotinylated to serve as the tether site for immobilization of DNA to the slide surface by biotin-streptavidin conjugation. The oligos were checked for appropriate emission signals by excitation of the Cy5 dye at 610 nm and by excitation of the Cy3 dye at 530 nm. Sets of the oligos were mixed in 20 mM Tris-HCl buffer to a final concentration of 20 uM and annealed using a personal Mastercycler (Eppendorf). DNA was stored at -20°C. DNA samples were serially diluted with buffer A (50 mM Tris, 50 mM NaCl, pH 8.0) to a final concentration of 10 pM. For DNA+GabR samples, GabR (5000 nM) was incubated with DNA at 25°C for 30 min in DNA binding buffer (20 mM Tris HCl, pH 8.0 50 mM KCl, 2 mM $MgCl_2$, 5% (vol/vol) glycerol, 1 mM EDTA, and 0.05% Nonidet P-40) then serially diluted with DNA binding buffer to a final DNA concentration of 10 pM. Flow chambers constructed from cleaned quartz slides (Technical Glass Products, Painesville, OH) were prepared for DNA immobilization by flowing 0.5 mg/mL BSA-biotin and streptavidin (0.1 mg/mL) with washes by buffer A. Solutions containing DNA or pre-incubated GabR-DNA complexes were then flowed through the chamber and allowed to incubate for 4 min. The sample was washed with DNA binding buffer and OSS buffer (25 mM Tris pH 8.0, 50 mM 8 mM Trolox, 5% glycerol, 1 mM EDTA, 1 mM DTT, 0.05% Nonident P-40, 50 mM KCl, 2 mM $MgCl_2$, 8% (m/v) glucose, 0.2 (mg/mL) glucose oxidase, 0.1 mg/mL catalase) was applied immediately before imaging to reduce photobleaching. The samples were imaged by prism-type total internal reflection with a 60X water

objective on an Olympus IX-83 with an EMCCD (Andor iXon DU897; Belfast, UK) cooled to -60°C. The Cy3 and Cy5 emission signals were spatially separated for simultaneous imaging by a series of dichroic mirrors (640 nm cutoff; Chroma Technologies, Bellow Falls, VT). Each pair of emission signals corresponding to the same molecule was identified using an affine transformation calibrated from a control slide coated with fluorescent fiducial markers. Data were acquired at 10 Hz. Data analysis was performed using custom Python software using established methodologies. FRET histograms were fit by Gaussian distributions using the Levenberg−Marquardt optimization with OriginPro (OriginLab, Northampton, MA).

Supplementary Material

The supplementary materials section provides a list of the synthesis protocols for all of the GABA analogs described in the series of compounds synthesized. The SI contains figures that were discussed in the main body of text, but not included because these figures are provide serve a supporting role to the main findings. The SI also includes alternate views to some figures to enhance display of experimental design and results.

Funding

The work was supported by NIH NIGMS R15GM113229 to DL and DB and by R01 DA030604 to RBS. This work made use of the IMSERC at Northwestern University, which has received support from the Soft and Hybrid Nanotechnology Experimental (SHyNE) Resource (NSF ECCS-1542205), the State of Illinois, and the International Institute for Nanotechnology (IIN).

REFERENCES

1. Belitsky BR, Sonenshein AL (2002) GabR, a member of a novel protein family, regulates the utilization of gamma-aminobutyrate in Bacillus subtilis. Mol Microbiol 45:569-583.

2. Belitsky BR (2004) Bacillus subtilis GabR, a protein with DNA-binding and aminotransferase domains, is a PLP-dependent transcriptional regulator. J Mol Biol 340:655-664.

3. Edayathumangalam R, Wu R, Garcia R, Wang Y, Wang W, Kreinbring CA, Bach A, Liao J, Stone TA, Terwilliger TC, Hoang QQ, Belitsky BR, Petsko GA, Ringe D, Liu D (2013) Crystal structure of Bacillus subtilis GabR, an autorepressor and transcriptional activator of gabT. Proc Natl Acad Sci USA 110:17820-17825.

4. Wu R, Sanishvili R, Belitsky BR, Juncosa JI, Le HV, Lehrer HJ, Farley M, Silverman RB, Petsko GA, Ringe D, Liu D (2017) PLP and GABA trigger GabR-mediated transcription regulation in Bacillus subtilis via external aldimine formation. Proc Natl Acad Sci USA 114:3891-3896.

5. Al-Zyoud WA, Hynson RM, Ganuelas LA, Coster AC, Duff AP, Baker MA, Stewart AG, Giannoulatou E, Ho JW, Gaus K, Liu D, Lee LK, Bocking T (2016) Binding of transcription factor GabR to DNA requires recognition of DNA shape at a location distinct from its cognate binding site. Nucleic Acids Res 44:1411-1420.

6. Amidani D, Tramonti A, Canosa AV, Campanini B, Maggi S, Milano T, di Salvo ML, Pascarella S, Contestabile R, Bettati S, Rivetti C (2017) Study of DNA binding and bending by Bacillus subtilis GabR, a PLP-dependent transcription factor. Biochim Biophys Acta Gen Subj 1861:3474-3489.

7. Park SA, Park YS, Lee KS (2017) Crystal structure of the C-terminal domain of Bacillus subtilis GabR reveals a closed conformation by gamma-aminobutyric acid binding, inducing transcriptional activation. Biochem Biophys Res Commun 487:287-291.

8. Slattery M, Zhou T, Yang L, Dantas Machado AC, Gordan R, Rohs R (2014) Absence of a simple code: how transcription factors read the genome. Trends Biochem Sci 39:381-399.

9. Rohs R, Jin X, West SM, Joshi R, Honig B, Mann RS (2010) Origins of specificity in protein-DNA recognition. Annu Rev Biochem 79:233-269.

10. Wilks JC, Kitko RD, Cleeton SH, Lee GE, Ugwu CS, Jones BD, BonDurant SS, Slonczewski JL (2009) Acid and base stress and transcriptomic responses in Bacillus subtilis. Appl Environ Microbiol 75:981-990.

11. Feehily C, Karatzas KA (2013) Role of glutamate metabolism in bacterial responses towards acid and other stresses. J Appl Microbiol 114:11-24.

12. De Biase D, Pennacchietti E (2012) Glutamate decarboxylase-dependent acid resistance in orally acquired bacteria: function, distribution and biomedical implications of the gadBC operon. Mol Microbiol 86:770-786.

13. Lee H, Doud EH, Wu R, Sanishvili R, Juncosa JI, Liu D, Kelleher NL, Silverman RB (2015) Mechanism of inactivation of gamma-aminobutyric acid aminotransferase by (1S,3S)-3-amino-4-difluoromethylene-1-cyclopentanoic acid (CPP-115). J Am Chem Soc 137:2628-2640.

14. Lee H, Le HV, Wu R, Doud E, Sanishvili R, Kellie JF, Compton PD, Pachaiyappan B, Liu D, Kelleher NL, Silverman RB (2015) Mechanism of inactivation of GABA aminotransferase by (E)- and (Z)-(1S,3S)-3-amino-4-fluoromethylenyl-1-cyclopentanoic acid. ACS Chem Biol 10:2087-2098.

15. Sarhan S, Knodgen B, Grauffel C, Seiler N (1993) Effects of inhibition of ornithine aminotransferase on thioacetamide-induced hepatogenic encephalopathy. Neurochem Res 18:539-549.

16. Liebschner D, Afonine PV, Moriarty NW, Poon BK, Sobolev OV, Terwilliger TC, Adams PD (2017) Polder maps: improving OMIT maps by excluding bulk solvent. Acta Cryst D73:148-157.

17. van Hijum SA, Medema MH, Kuipers OP (2009) Mechanisms and evolution of control logic in prokaryotic transcriptional regulation. Microbiol Mol Biol Rev 73:481-509.

18. Lee DJ, Minchin SD, Busby SJ (2012) Activating transcription in bacteria. Annu Rev Microbiol 66:125-152.

19. Browning DF, Busby SJ (2004) The regulation of bacterial transcription initiation. Nat Rev Microbiol 2:57-65.

20. Busby SJW, Savery NJ (2007) Transcription Activation at Bacterial Promoters. In Encyclopedia of Life Sciences, John Wiley & Sons: Chichester.

21. Okuda K, Kato S, Ito T, Shiraki S, Kawase Y, Goto M, Kawashima S, Hemmi H, Fukada H, Yoshimura T (2015) Role of the aminotransferase domain in Bacillus subtilis GabR, a pyridoxal 5'-phosphate-dependent transcriptional regulator. Mol Microbiol 95:245-257.

22. Brown NL, Stoyanov JV, Kidd SP, Hobman JL (2003) The MerR family of transcriptional regulators. FEMS Microbiol Rev 27:145-163.

23. Molina-Henares AJ, Godoy P, Duque E, Ramos JL (2009) A general profile for the MerR family of transcriptional regulators constructed using the semi-automated Provalidator tool. Environ Microbiol Rep 1:518-523.

24. Hobman JL (2007) MerR family transcription activators: similar designs, different specificities. Mol Microbiol 63:1275-1278.

25. Heldwein EE, Brennan RG (2001) Crystal structure of the transcription activator BmrR bound to DNA and a drug. Nature 409:378-382.

26. Winn MD (2003) An overview of the CCP4 project in protein crystallography: an example of a collaborative project. J Synchrotron Radiat 10:23-25.

27. Adams PD, Grosse-Kunstleve RW, Hung LW, Ioerger TR, McCoy AJ, Moriarty NW, Read RJ, Sacchettini JC, Sauter NK, Terwilliger TC (2002) PHENIX: building new software for automated crystallographic structure determination. Acta Cryst D58:1948-1954.

28. Emsley P, Lohkamp B, Scott WG, Cowtan K (2010) Features and development of Coot. Acta Cryst D66:486-501.

29. Paettersen E, Goddard T, Huang C, Couch G, Greenblatt D, Meng E, Ferrin T (2004) UCSF Chimera--a visualization system for exploratory research and analysis. J Comput Chem 25:1605-1612.

30. Koo YK, Nandi D, Silverman RB (2000) The multiple active enzyme species of gamma-aminobutyric acid aminotransferase are not isozymes. Arch Biochem Biophys 374:248-254.

31. Mascarenhas R, Le HV, Clevenger KD, Lehrer HJ, Ringe D, Kelleher NL, Silverman RB, Liu D (2017) Selective targeting by a mechanism-based inactivator against pyridoxal 5'-phosphate-dependent enzymes: Mechanisms of inactivation and alternative turnover. Biochemistry 56:4951-4961.

32. Le HV, Hawker DD, Wu R, Doud E, Widom J, Sanishvili R, Liu D, Kelleher NL, Silverman RB (2015) Design and mechanism of tetrahydrothiophene-based gamma-aminobutyric acid aminotransferase inactivators. J Am Chem Soc 137:4525-4533.

33. Juncosa JI, Lee H, Silverman RB (2013) Two continuous coupled assays for ornithine-delta-aminotransferase. Anal Biochem 440:145-149.

34. Zigmond E, Ben Ya'acov A, Lee H, Lichtenstein Y, Shalev Z, Smith Y, Zolotarov L, Ziv E, Kalman R, Le HV, Lu H, Silverman RB, Ilan Y (2015) Suppression of hepatocellular carcinoma by inhibition of overexpressed ornithine aminotransferase. ACS Med Chem Lett 6:840-844.

Table 1. Statistics of crystal structure of GabR-PGP

Data Processing:	
Space group	P 4_12_12
Cell dimension	
α, β, γ (deg)	152.65, 152.65, 69.16
a, b, c (Å)	90, 90, 90
Resolution (Å)	2.80
Resolution at I/σ (I) =2	
R_{merge} [a] (%)	9.3 (3.7)[b]
R_{pim} [c] (%)	4.7 (0.0)
I/σ (I)	11.2 (1.8)
CC ½ [d]	99.7
Completeness (%)	100 (100)
Multiplicity	4.8
No. Reflections	99252
No. Unique Reflections	20715
Refinement:	
R_{work} [e]/R_{free} [f](%)	17.31/20.18
No. of Atoms	
protein	9616
ligand	89
water	1121
B factors (Å^2)	
protein	28.0
RMSD [g]	
bond lengths (Å)	0.004
bond angles (deg)	0.72
Ramachandran plot (%)	
favored	96.27
allowed	3.48
outliers	0.25

[a]Rmerge = Σ|Iobs − Iavg|/ΣIavg
[b]The values for the highest-resolution bin are in parentheses
[c]Precision-indicating merging R
[d]Pearson correlation coefficient of two "half"data sets
[e]Rwork = Σ|Fobs − Fcalc|/ΣFobs

[f]Five percent of the reflection data were selected at random as a test set, and only these data were used to calculate Rfree
[g]Root-mean square deviation
[h]Not applicable

Scheme 1. Preparation of 4-phenoxymethyl-GABA **13** and derivatives

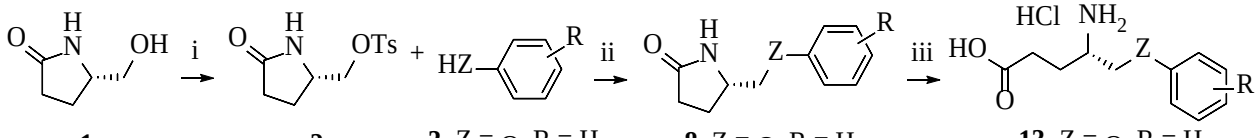

1 **2**

3; Z = O, R = H
4; Z = O, R = 2-F
5; Z = O, R = 3-F
6; Z = O, R = 4-F
7; Z = S, R = H

8; Z = O, R = H
9; Z = O, R = 2-F
10; Z = O, R = 3-F
11; Z = O, R = 4-F
12; Z = S, R = H

13; Z = O, R = H
14; Z = O, R = 2-F
15; Z = O, R = 3-F
16; Z = O, R = 4-F
17; Z = S, R = H

[a]Reagents and conditions: (*i*) TsCl, Et_3N, catalytic DMAP, CH_2Cl_2, 20 h, rt; (*ii*) K_2CO_3, CH_3CN, 20 h, 115 °C; (*iii*) HCl 3 h, 110 °C.

Scheme 2. GabR facilitates the formation of PGP from **PLP** and **13**

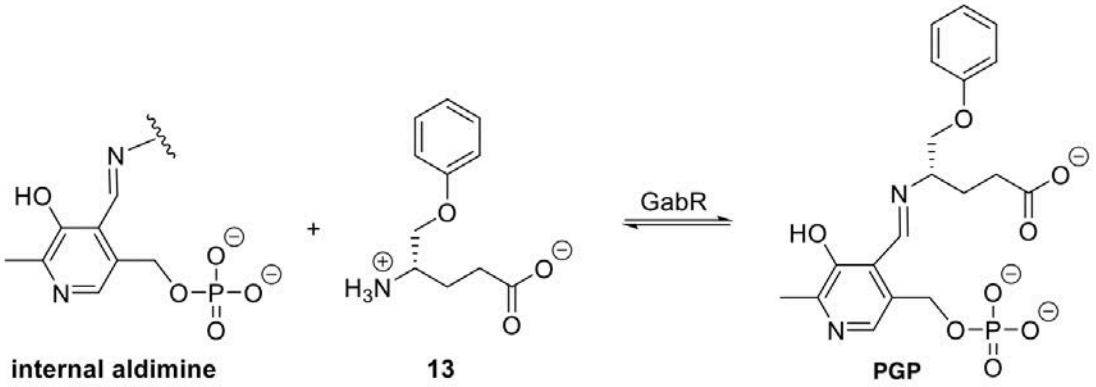

Figure Captions

Figure 1. Binding region and structure of GabR. (a) Schematic of GabR binding site on the gabR and gabTD promoters. (b) Surface/Ribbon diagram of the GabR homodimer. Chain A is shown in blue while the C-terminal eb/o and N-terminal wHTH domains of chain B are depicted in maroon ribbon and surface representations. The tether segment (His114-Glu81) connecting the C- and N-terminal domains of chain B is colored orange.

Figure 2. PLP-**13** (PGP) interactions in the binding site of GabR (PDB 6UXZ). (a) Interactions between the side chain residues of GabR involved in substrate recognition including the carboxylate of PGP. (b) A superimposition of the external aldimine PLP-GABA in magenta (PDB code: 5T4J) and the external aldimine PGP in tan with surrounding residues in the binding site.

Figure 3. A polder map (F_o-F_c) of PGP. The polder map is shown as a grey mesh at 3.0σ. The polder map was generated by extracting the PGP structure from the coordinates.

Figure 4. Screening for potential off-target aminotransferase activity of *h*OAT, Asp-AT, GABA-AT, and Ala-AT in the presence of **13-16**.

Figure 5. smFRET distribution curves. Observed smFRET distribution for (a) DNA only, (b) DNA + GabR, (c) DNA + GabR + GABA, and (d) DNA + GabR + **13**. Curves were fit by multimodal using Gaussian distributions. See Table S1 for fitting parameters.

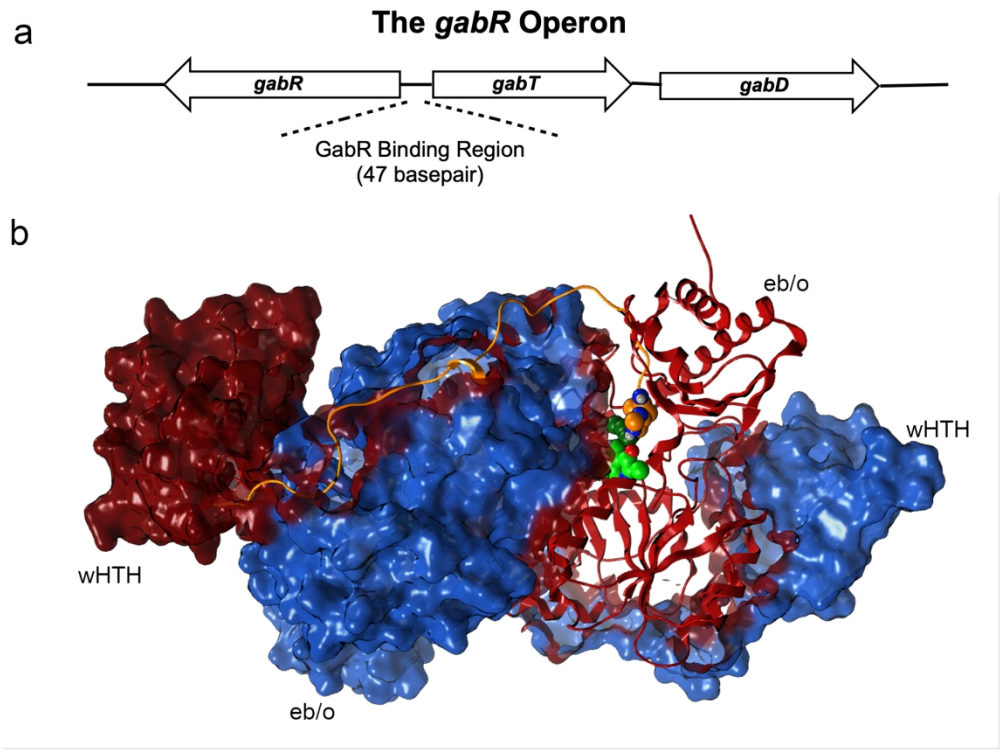

Figure 1. Binding region and structure of GabR. (a) Schematic of GabR binding site on the gabR and gabTD promoters. (b) Surface/Ribbon diagram of the GabR homodimer. Chain A is shown in blue while the C-terminal eb/o and N-terminal wHTH domains of chain B are depicted in maroon ribbon and surface representations. The tether segment (His114-Glu81) connecting the C- and N-terminal domains of chain B is colored orange.

677x508mm (72 x 72 DPI)

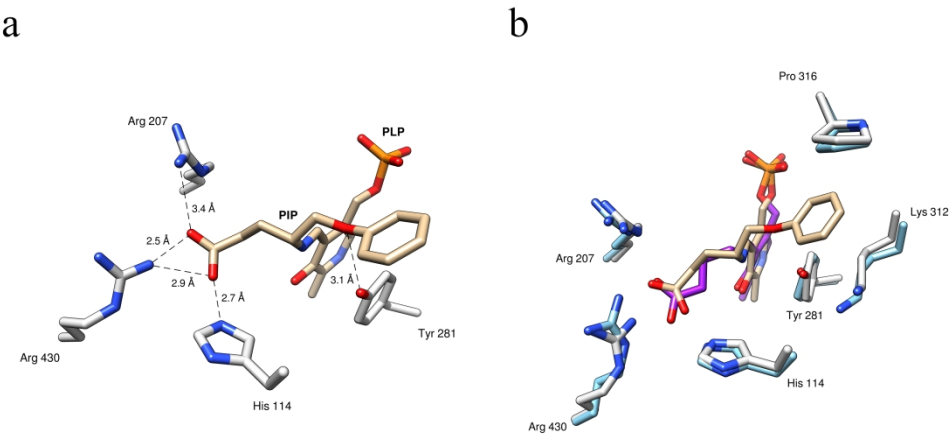

Figure 2. PLP-13 (PGP) interactions in the binding site of GabR (PDB 6UXZ). (a) Interactions between the side chain residues of GabR involved in substrate recognition including the carboxylate of PGP. (b) A superimposition of the external aldimine PLP-GABA in magenta (PDB code: 5T4J) and the external aldimine PGP in tan with surrounding residues in the binding site.

304x151mm (300 x 300 DPI)

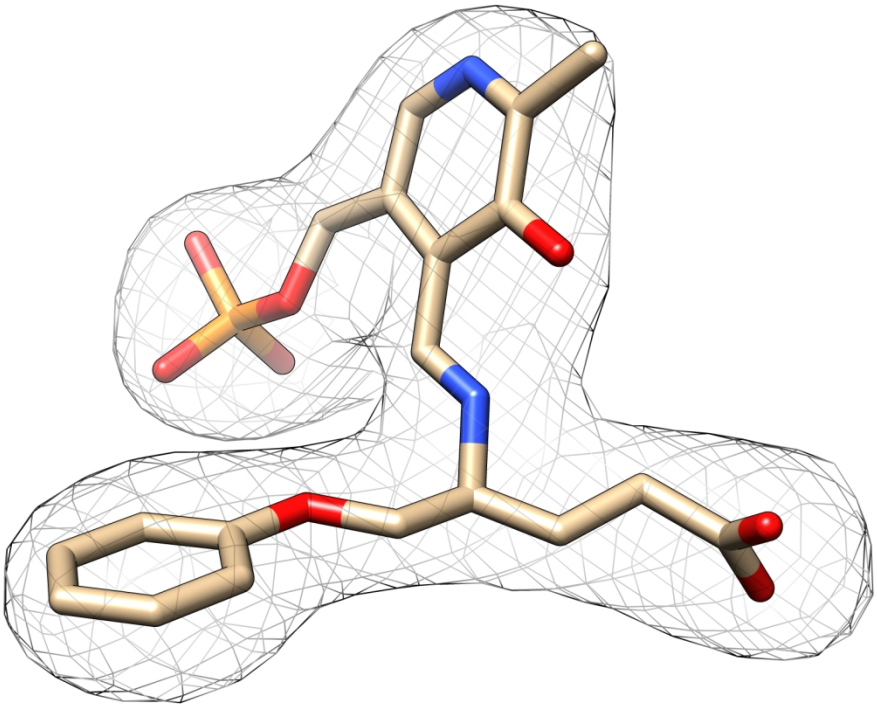

Figure 3. A polder map (Fo-Fc) of PGP. The polder map is shown as a grey mesh at 3.0 sigma. The polder map was generated by extracting the PGP structure from the coordinates.

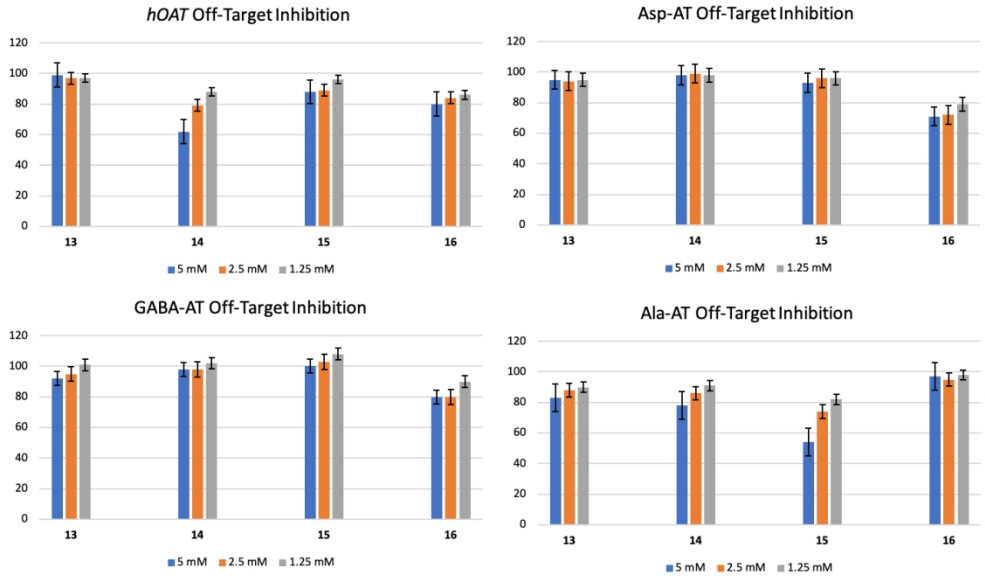

Figure 4. Screening for potential off-target aminotransferase activity of hOAT, Asp-AT, GABA-AT, and Ala-AT in the presence of 13-16.

510x309mm (72 x 72 DPI)

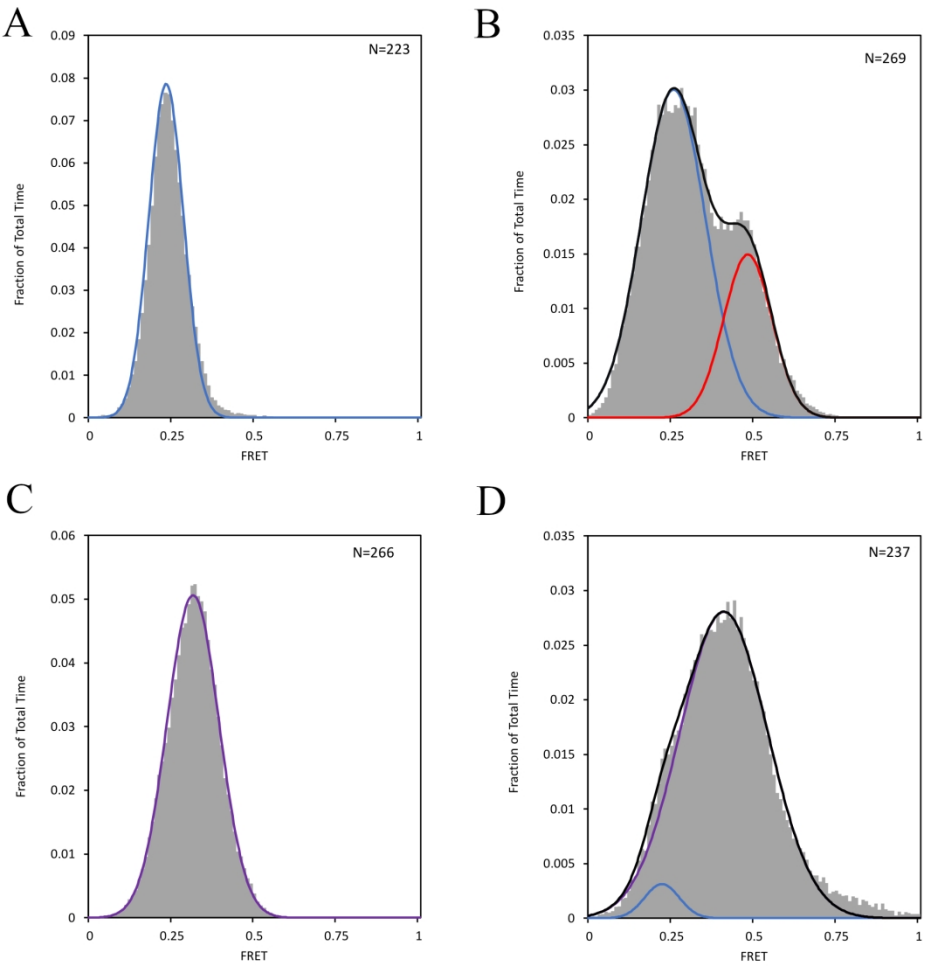

Figure 5. smFRET distribution curves. Observed smFRET distribution for (a) DNA only, (b) DNA + GabR, (c) DNA + GabR + GABA, and (d) DNA + GabR + 13. Curves were fit by multimodal using Gaussian distributions. See Table S1 for fitting parameters.

177x177mm (300 x 300 DPI)